Oblivious Processing in a Fronthaul Constrained Gaussian Channel

Adi Homri, Michael Peleg and Shlomo Shamai

September 28, 2016

Abstract

We consider systems for which the transmitter conveys messages to the receiver through a capacity-limited relay station. The channel between the transmitter and the relay-station is assumed to be frequency selective additive Gaussian noise channel. It is assumed that the transmitter can shape the spectrum and adapt the coding technique as to optimize performance. The relay operation is oblivious(nomadic transmitters [1]), that is, the specific codebooks used are unknown, while the spectral shape of the transmitted signal is available. We find the reliable information rate that can be achieved in this setting with Gaussian signaling, and to that end employ Gaussian bottleneck results [2] combined with Shannon's incremental frequency approach [3]. We also prove that unlike classical water-pouring, the allocated spectrum(power and bit-rate) of the optimal solution could be frequently discontinuous.

arXiv:1510.08202v2 [cs.IT] 26 Sep 2016

1 Introduction

The relaying technique makes use of intermediate nodes to help the communication between two distant nodes. Elementary relaying can be coarsely divided into compress-and- forward (amplify-and-forward is viewed as a special case) and decode-and-forward, depending on whether the relays decode the transmitted message or just forward the received signal to the destination. In this paper we examine the "oblivious" relay system. The oblivious approach is intended to construct universal relaying components serving many diverse users and operators and *not dependent on knowing the modulation method and coding.* Such an approach might benefit systems used in 'cloud' communication and was investigated for example in [4].

Figure 1 The oblivious relay serving a user - Gaussian vector channel

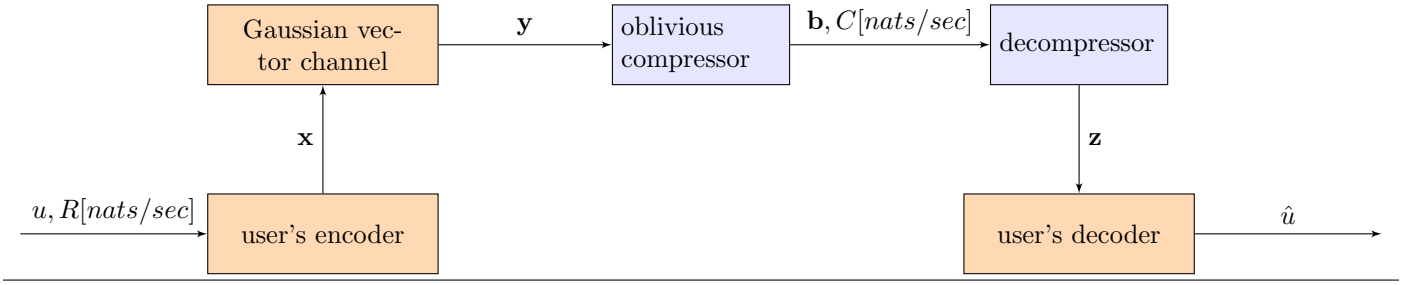

Consider the system in Figure 1. The relay that compresses the received signal and forwards it to the final user's destination by a finite rate link provides the user with a memoryless communication channel forwarding symbols from the transmitter to the receiver. The user transmits the symbols $\mathbf{x}$ and receives symbols $\mathbf{z}$ while the effective channel is governed by the transition probability $P(\mathbf{z}|\mathbf{x})$. We choose $\mathbf{x}$ to be Gaussian because of its optimality at large C and because of its ubiquitous applications. In such a setting the user faces the familiar memoryless communication channel and can choose freely how to utilize it, e.g. selecting a good error correcting code and changing the codes after the oblivious system was already implemented. The serving system is oblivious of the channel code used. See [1] for a more rigorous presentation of obliviousness. The relay performs lossy compression of the output of the Gaussian channel. The trade-off between compression rate and mutual information between channel input and compressed channel output has closed-form expressions for the scalar and vector case using the Gaussian Information Bottleneck(GIB) theorem [2, 5] and [6]. This deviates from the classical remote rate distortion approach [7], [8] and [9](rate distortion for sub-Nyquist sampling scheme) and [10](Sampling stationary signals subject to bit-rate constraints), since the distortion is measured by the equivocation $H(X|Z)$ and not $MMSE = E(X-Z)^2$. Say the distribution of X is fixed, then minimizing $H(X|Z)$ means maximizing $I(X;Z) = H(X) - H(X|Z)$. In this paper, we provide a further generalization of the GIB for the case of frequency selective additive Gaussian. We find the reliable information rate that can be achieved in this setting, and to that end employ Gaussian bottleneck results [2] combined with Shannon's incremental frequency approach [3].

The reminder of this paper is organized as follows. Section 3 provides the required background and definitions for the GIB. In Section we look into quantization alternatives. In Section 4, we review the main results relevant to frequency-flat channel from [5, 3] and present the new derivation for frequency selective channel and infinite-processing-time. Numerical results are provided in Section 5, conclusions and future discussions on 6. *Notation:* We use boldface letters for column vectors and sequences. The expectation operator is denoted by E and we follow the notation of [11] for entropy $H(\cdot)$, differential entropy $h(\cdot)$, and mutual information $I(\cdot;\cdot)$. Furthermore, $[x]^+ \triangleq \max\{x, 0\}$. All logarithms are natural.

2 Quantization Alternatives

Denote by x, y, z the channel input, the received signal and the quantized output respectively. Our system will try to maximize $I(x_i; z_i)$ which clearly determine the maximal information rate R of the whole system if the user utilizes good error correcting codes while minimizing the bitrate of the sequence **b**. Here we list some possible approaches to quantization:

2.1 Using the channel code in the serving subsystem

If the serving subsystem would not be oblivious, it would decode the original information ($\hat{u}$) and send it as the sequence **b**. In this case R=min(C, radio channel capacity) would be achieved. But in this work the serving subsystem is oblivious.

2.2 Memoryless deterministic quantizer

The received signal y is mapped to a discrete valued variable z by a deterministic function. The function is optimized for Mutual Information (MUI), $I(x; z)$ per symbol with a constraint on the number of bits required to represent the quantizer output symbol. The optimization can be done by the Lloyd algorithm. This is well covered by published papers, e.g.[12] which also shows the optimal PDF of the transmitted signal x is discrete in many cases. Entropy compression such as the Huffman scheme is added after the quantizer as suggested in the literature.

2.3 Stochastic quantizer

The performance can be improved if we allow the quantizer to be stochastic, as mentioned for example in [13]. In principle, for each channel output y_i a compressed representation z_i is obtained by a stochastic quantizer characterized by $P(z_i|y_i)$ chosen to maximize $I(x_i; z_i)$, then z_i is compressed and sent to the users decoder using the bit rate $C = I(y_i; z_i)$. The practical implementation is by means of source coding on sequences. The received sequence **y** is encoded into the sequence of bits **b** and the destination recovers the sequence **z** from **b**. The serving system bit rate can be limited to $C = I(y_i; z_i)$. A proof following the steps of the source coding theorem [11] can be constructed. The PDF $P(z_i|y_i)$ will set $I(x_i; z_i)$ and thus enable system communication rate of $R = I(x_i; z_i)$ by the classic channel coding theorem.

Letting the quantizer be stochastic improves performance similarly to a corresponding advantage of source coding over memoryless deterministic quantization [11].

The stochastic quantizer for the Gaussian signals is analyzed in [5] . Koch [14] is another paper on stochastic quantizer, the randomness there is limited to dither known to the quantizer, this is a special case and may be considered a deterministic time-varying quantizer. The quantizer optimization problem is now the bottleneck style problem, e.g. [15], of maximizing $I(x_i; z_i)$ with a constraint on $I(y_i; z_i)$. Next we shall present some attributes of the stochastic quantizer.

2.4 Demonstrating the advantages of the stochastic quantizer

The advantage of the stochastic quantizer is demonstrated by a numerical example, see Figure 2. We examine the case of Gaussian x over AWGN channel with quantization rate $C = 1$[bits/symbol]. In the deterministic quantizer case, the quantizer is the sign of the received signal . The curve in Figure 2 is the numerical evaluation of $E_{x,z} log \frac{P(z|x)}{P(z)}$. In the stochastic case we have from [5]

$$I(w; v) = \frac{1}{2} log \left(\frac{1 + a}{1 + ae^{-2c}} \right) \tag{1}$$

The results in Figure 2 show the clear superiority of the stochastic quantization over the deterministic one. Modifying the distribution of x would improve the rate [12], see the improved performance with a binary input in Figure 2.

Figure 2 Mutual information and system information rate R with Gaussian signal and two quantizers over the AWGN channel and quantization rate of $C = 1$bit/channel use. Binary input is also examined for comparison.

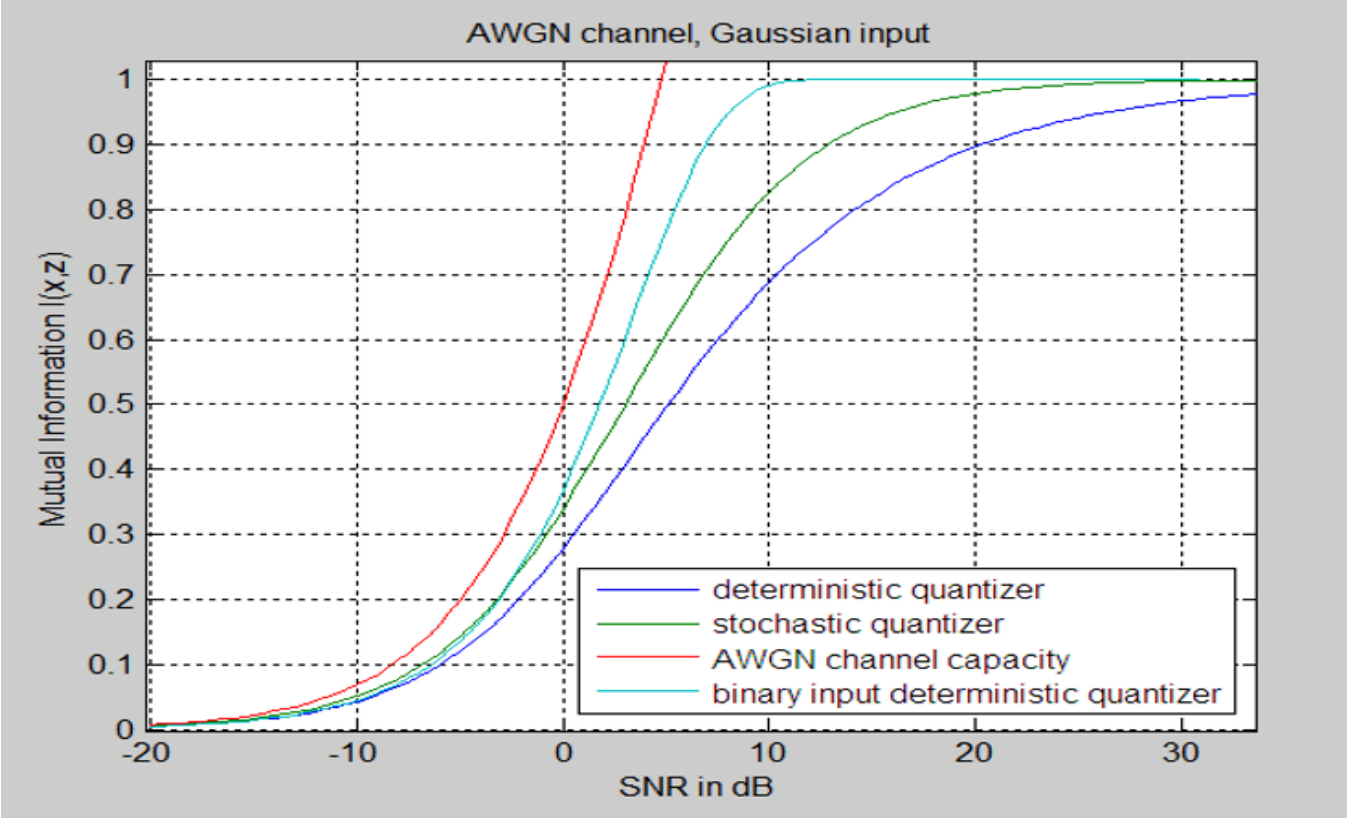

2.5 Independent z_i achieve the optimal performance

We might still wonder if the stochastic quantizer, while evidently better than the deterministic one, is optimal. That is, the z_i in our scheme are statistically independent. Could this scheme be outperformed if dependence between the z_i was permitted? For example the channel from x to y could be a BSC and the relay could convey information to the destination by setting z_i to be parity bits obtained by the XOR operation on pairs of y_i. We shall show next that the independent z_i, each statistically dependent on a single y_i only, achieve the best performance possible. To show this, we consider the scheme as in Figure 1 but instead of producing $\mathbf{z}$, the bit sequence $\mathbf{b} = \mathbf{z}$ is derived directly from the sequence $\mathbf{y}$ and passed to the decoder together with the compression scheme. Thus we want to maximize $I(\mathbf{x};\mathbf{z})$, that is MUI of whole sequences, with a constraint on $I(\mathbf{y};\mathbf{z})$, because the first term is the information rate of the whole system and the second term is an achievable lower bound on the backhaul bitrate C. We can restate this question as an equivalent bottleneck problem: Let $\mathbf{x},\mathbf{y},\mathbf{z}$ be sequences comprising each N elements x_i, y_i, z_i. Also the elements of $\mathbf{x},\mathbf{y}$ be i.i.d. and the channel $\mathbf{x} \quad - \quad \mathbf{y}$ is memoryless. We want to solve the bottleneck problem:

$$\text{Find } P(\mathbf{z}|\mathbf{y}) \text{ which maximizes } I(\mathbf{z};\mathbf{x}) \text{ with a constrained } I(\mathbf{y};\mathbf{x}) \ ,$$

$$Is\ P(\mathbf{z}|\mathbf{y}) = \Pi_i P(z_i|y_i)\ ? \tag{2}$$

The answer was already proved positive by Witsenhausen and Wyner [16] for discrete alphabets of x, y and also for Gaussian x over the AWGN channel the answer was already proved positive in Tishbi [15]. Proof for general x and general channels is presented in the appendix.

Theorem 1. *The bottleneck problem has an optimal solution for which the independence of z_i holds, as defined by (2)*

2.6 Discrete channel output

In most practical systems the channel output y will be converted to a digital form before any processing. This will produce discrete-valued y. It is proved in [16] that with discrete alphabets of x, y an optimal z exists which is discrete and of cardinality exceeding that of y by at most one. A proof valid also for continuous x is presented in the appendix

3 Gaussian Information Bottleneck

3.1 Information rate - vector channel

The Gaussian Information Bottleneck and its derivation for the discrete-time signaling case, was thoroughly studied at [5, 15, 2, 6] and [17]. We will now give a brief overview of the GIB (the interested reader is referred to [5, 6] for a full

treatment). A complete derivation of the information rate function for the vector case, as well as the difference between the information rate function and the rate-distortion function namely, $I(R) \geq I^{RD}(R)$, is presented in [6].

Figure 3 Gaussian Information Bottleneck - Vector Case

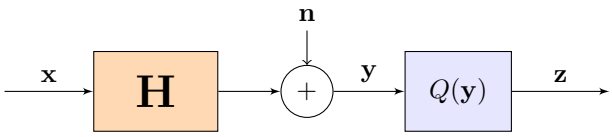

Consider the system in Figure 3. Let $\mathbf{x}$ and $\mathbf{y}$ be jointly Gaussian zero-mean random vectors(length n) with full rank covariance matrices. Assuming that $\mathbf{x} \sim \mathcal{N}(\mathbf{0}, \mathbf{R_{xx}})$. The channel output equals

$$\mathbf{y} = \mathbf{H}\mathbf{x} + \mathbf{n} \tag{3}$$

where $\mathbf{H} \in \mathcal{R}^{n \times m}$ and the additive noise $\mathbf{n} \sim \mathcal{N}(\mathbf{0}, \sigma^2\mathbf{I})$ is independent of $\mathbf{x}$ which results

$$\mathbf{R_{yy}} = \mathbf{H}\mathbf{R_{xx}}\mathbf{H^T} + \sigma^2\mathbf{I} \tag{4}$$

Let $\mathbf{z}$ be a compressed representation of $\mathbf{y}$ denoted by the conditional distribution $P(\mathbf{z}|\mathbf{y})$. It follows that $\mathbf{x} - \mathbf{y} - \mathbf{z}$ forms a Markov chain and hence by Markovity

$$P(\mathbf{z}|\mathbf{x}) = \int_{\mathcal{R}^n} P(\mathbf{z}|\mathbf{y})P(\mathbf{y}|\mathbf{x})d\mathbf{y} \tag{5}$$

The compression rate equals $I(\mathbf{z};\mathbf{y})$. The GIB addresses the following variational problem [13]:

$$\min_{P(\mathbf{z}|\mathbf{y})} I(\mathbf{z};\mathbf{y}) - \beta I(\mathbf{x};\mathbf{z}) \tag{6}$$

In the context of the information bottleneck method, $\mathbf{x}$ is called the *relevance variable* and $I(\mathbf{x};\mathbf{z})$ is termed *relevant information*. The trade-off between compression rate and relevant information is determined by the positive parameter β. It has been shown that the optimal $\mathbf{z}$ is jointly Gaussian with $\mathbf{y}$ and can be written as

$$\mathbf{z} = \mathbf{A}\mathbf{y} + \xi \tag{7}$$

where $\mathbf{A}$ is an $n \times n$ matrix and $\xi \sim \mathcal{N}(\mathbf{0}, \mathbf{C}_\xi)$ is independent of $\mathbf{y}$.

Definition 1. *Let $\mathbf{x} - \mathbf{y} - \mathbf{z}$ be a Markov chain. The information-rate function $I : \mathcal{R}_+ \to [0, I(\mathbf{x};\mathbf{y})]$ is defined by [5]*

$$I(C) \triangleq \max_{P(\mathbf{z}|\mathbf{y})} I(\mathbf{x};\mathbf{z}) \text{ subject to } I(\mathbf{y};\mathbf{z}) \leq C \tag{8}$$

$I(C)$ quantifies the maximum of the relevant information that can be preserved when the compression rate is at most C.

3.2 Information rate - scalar channel

We now present $I(C)$ for the channel depicted at Figure 3 for the scalar case. Since x and y are real zero-mean jointly Gaussian random variables, they obey:

$$y = \sqrt{h}x + n \tag{9}$$

where $h \in \mathcal{R}_+$ and $n \sim \mathcal{N}(0, \sigma^2)$ is independent of x. Setting $x \sim \mathcal{N}(0, P)$ yields $y \sim \mathcal{N}(0, hP + \sigma^2)$. The compressed representation of y is denoted $z = Q(y)$. By Markovity of $x - y - z$ we have

$$P(z|x) = \int_{\mathcal{R}} P(z|y)P(y|x)dy \tag{10}$$

where $P(y|x)$ is the transition pdf of the Gaussian channel and $P(z|y)$ describes the compression mapping Q. The capacity of the Gaussian channel $P(y|x)$ with average power constraint P and no channel compression equals [11](units are [nats/channel use])

$$\mathcal{C}(\rho) \triangleq \frac{1}{2}log(1 + \rho) \tag{11}$$

with ρ as the signal-to-noise ratio (SNR)

$$\rho \triangleq \frac{hP}{\sigma^2} \tag{12}$$

The following corollary states a closed-form expression for the information-rate function and properties [5, Theorem 2].

Corollary 1. *The information-rate function of a Gaussian channel with SNR ρ is given by*

$$I(C) = \frac{1}{2} log\left(\frac{1+\rho}{1+\rho e^{-2C}}\right) \tag{13}$$

$I(C)$ has the following properties:

(a) $I(C)$ *is strictly concave in* $\mathcal{R}_+$

(b) $I(C)$ *is strictly increasing in* C.

(c) $I(C) \leq min\{C, \mathcal{C}(\rho)\}$

(d) $I(0) = 0$ *and* $\lim_{C\to\infty} I(C) = \mathcal{C}(\rho)$

(e) $\frac{\partial I(C)}{\partial C} = (1 + e^{2C}\rho^{-1})^{-1} \leq \frac{\partial I(C)}{\partial C}|_{C=0} = (1+\rho^{-1})^{-1}$

The proof is within [5], It should be noted that it can also be proved using the I-MMSE relation [18, Chapter 5, Section 7.1.3].

Figure 4 $I(x;z)$ vs. Rate and ρ(SNR)

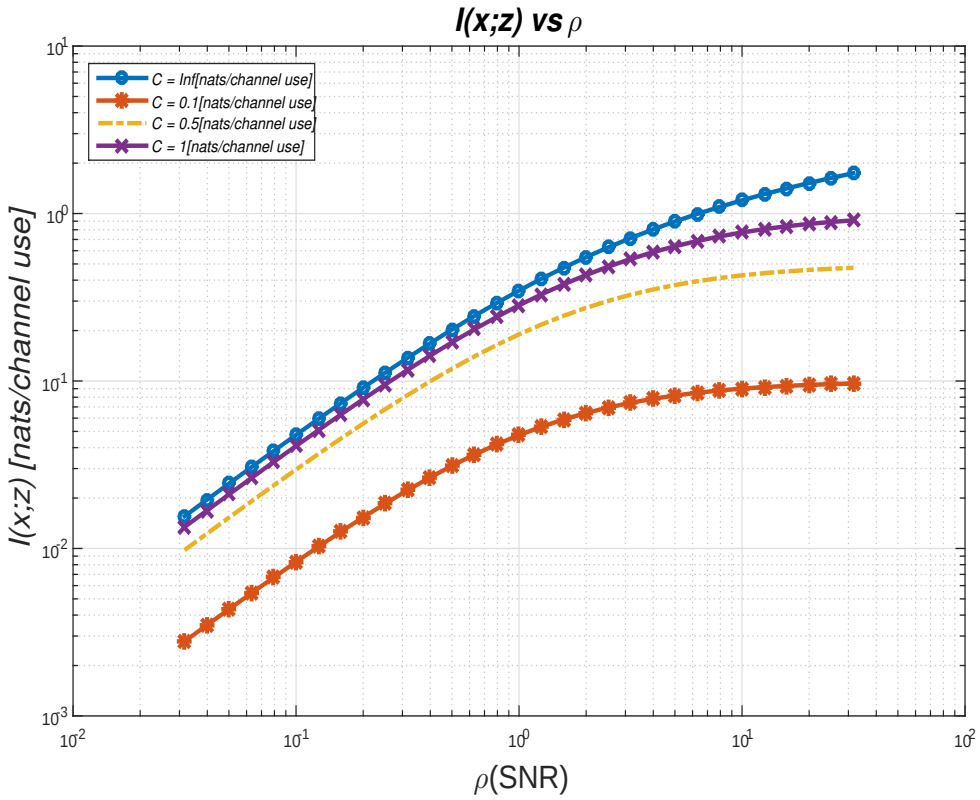

Figure 4 illustrates the effect of limited-rate processing. It is clear the that the total mutual information is upper bounded by the capcity for AWGN channels (which can be achieved by the water-pouring approach) presented by Shannon [3].

4 Generalizing the GIB - Frequency Selective Channel Infinite Processing Time

Figure 5 Finite rate fronthaul Gaussian channel

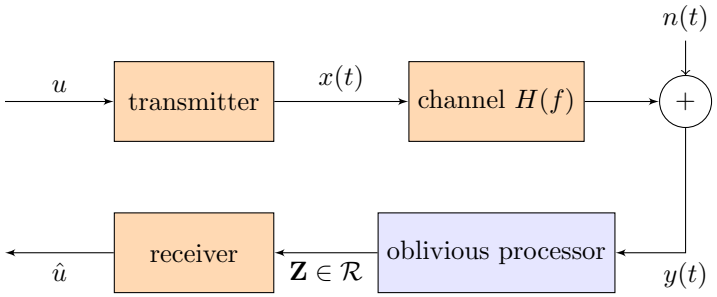

Consider the system depicted in figure 5. $x(t)$ - the input signal assumed to be Gaussian, $H(f)$ - the frequency response of the channel linear filter, and impulse response $\mathcal{F}^{-1}(H(f)) = h(t)$ (here, $\mathcal{F}, \mathcal{F}^{-1}$ designate the Fourier response and its inverse)

$$y(t) = x(t) * h(t) + n(t) \tag{14}$$

where $n(t)$ is a normalized additive white Gaussian noise with one-sided power spectral density $N_0 = 1[Watt/Hz]$, and $*$ designates convolution.

We are interested in the normalized mutual-information when standard coding theorems [19] guarantee that the associated rate can be reliably transmitted through the system.

$$\lim_{T\to\infty} \frac{1}{2T} I\left(X_{-T}^{T}; \mathbf{Z}\right) \triangleq I_n^C(x;z) \tag{15}$$

where $x_a^b : (x(t), a \le t \le b)$ and where $\mathbf{Z}$ is the output binary vector that is constrained to be $\mathcal{C}$[nats/sec], The information in (15) is also measured in terms of [nats/sec]. n denotes the n-symbol block transmitted and is the dimension of $\mathbf{Z}$.

Again, we'd like to find the(one-sided) power spectral density of the input Gaussian process $S_x(f)$ which maximizes $I_n^C(x;z)$ under an average power constraint under some bandwidth W:

$$\int_0^W S_x(f)df \le P \tag{16}$$

4.1 Water pouring

First we shall recall the classical water pouring approach which yields the maximum $I_n^\infty(x;z)$ for $C \to \infty$.

The idea of splitting the channel into incremental bands appears in [3] and [11] where each incremental band of bandwidth df is treated as ideal (independent due to Gaussianity) band-limited channel with response $H(f)df$, and the result yields:

$$\lim_{C\to\infty} I_n^C(x;z) \triangleq I_n^\infty(x;z) = \int_0^W log\left[1 + S_x(f)|H(f)|^2\right]df \tag{17}$$

Optimizing this over $S_x(f)$ under the power constraint yields (using the standard Euler-Lagrange [20])

$$\frac{|H(f)|^2}{1 + S_x(f)|H(f)|^2} = \frac{1}{b} \tag{18}$$

Thus, the result is (see [3, chapter 8]).

$$I_{water-pouring} \triangleq I_n^\infty(x;z) = \int_{\mathcal{B}} log\left[b|H(f)|^2\right]df \tag{19}$$

and where the frequency region $\mathcal{B}$ is given by

$$\mathcal{B} = \{f : b - \frac{1}{|H(f)|^2} \ge 0\} \tag{20}$$

4.2 Processing under limited bit-rate C

As before, we adopt the Shannon's incremental view taking advantage of the fact that disjoint frequency bands are independent under the Gaussian law and stationarity . Let $\frac{1}{2}C(f)$ designate the number of [nats/channel use] assigned for delivering (processing) the band $(f, f+df)$. Since we do have $2df$ independent channel uses (Nyquist) per second, the total rate per second in each band is

$$\frac{1}{2}C(f)2df = C(f)df$$

and hence,

$$\int_0^W C(f)df = C \tag{21}$$

culminating this view and incorporating (13), we reach the equation:

$$I[f, S_x(f), C(f)] = \int_0^W log\left[1 + S_x(f)|H(f)|^2\right]df - \int_0^W log\left[1 + S_x(f)|H(f)|^2 e^{-C(f))}\right]df \tag{22}$$

$$\max_{S_x(f), C(f)} \int_0^W log\left(\frac{1 + S_x(f)|H(f)|^2}{1 + S_x(f)|H(f)|^2 e^{-C(f)}}\right)df \; s.t. \quad \int_0^W S_x(f)df = P, \int_0^W C(f)df = C \tag{23}$$

The result follows the standard Euler-Lagrange [20] reasoning. To that end, we follow the notation presented in [20]. Assuming $I[f,\hat{S}_x,\hat{C}] \triangleq log\left(\frac{1+S_x(f)|H(f)|^2}{1+S_x(f)|H(f)|^2e^{-C(f)}}\right)$, is the mutual information spectral density[nats/sec/Hz]. Also, $\hat{S}_x \triangleq S_x(f)$,$\hat{C} \triangleq C(f)$. The Lagrangian is:

$$L\left[f,\hat{S}_x,\hat{C}\right] = I[f,\hat{S}_x,\hat{C}] - \lambda_c \cdot \hat{C} - \lambda_s \cdot \hat{S}_x \qquad ,\{\lambda_c,\lambda_s\} \in \Re \tag{24}$$

Differentiating $L\left[f,\hat{S}_x,\hat{C}\right]$ with respect to $\hat{C},\hat{S}_x$ leads:

$$\frac{\partial I[f,\hat{S}_x,\hat{C}]}{\partial \hat{S}_x} - \lambda_s = 0 \tag{25a}$$

$$\frac{\partial I[f,\hat{S}_x,\hat{C}]}{\partial \hat{C}} - \lambda_c = 0 \tag{25b}$$

$$\frac{H(f)^2(1-e^{-\hat{C}})}{(1+\hat{S}_xH(f)^2)(1+\hat{S}_xH(f)^2e^{-\hat{C}})} - \lambda_s = 0 \tag{26a}$$

$$\frac{\hat{S}_xH(f)^2e^{-\hat{C}}}{1+\hat{S}_xH(f)^2e^{-\hat{C}}} - \lambda_c = 0 \tag{26b}$$

Proposition 1. *$\{\lambda_c,\lambda_s\}$ are bounded by:*

$$0 \le \lambda_s \le \max H(f)^2 \quad , \quad 0 \le \lambda_c \le 1 \tag{27}$$

Proof. By investigating the derivatives of $I[f,\hat{S}_x,\hat{C}]$ w.r.t $\{\hat{S}_x,\hat{C}\}$ and taking into account that $\hat{S}_x \ge 0, \hat{C} \ge 0$ one can see that

$$\lambda_s = \frac{\partial I[f,\hat{S}_x,\hat{C}]}{\partial \hat{S}_x} = \frac{H(f)^2(1-e^{-\hat{C}})}{(1+\hat{S}_xH(f)^2e^{-\hat{C}})(1+\hat{S}_xH(f)^2)} > 0 \tag{28a}$$

$$\lambda_s = \frac{\partial I[f,\hat{S}_x,\hat{C}]}{\partial \hat{S}_x} \le H(f)^2 \le \max H(f)^2 \tag{28b}$$

$$\lambda_c = \frac{\partial I[f,\hat{S}_x,\hat{C}]}{\partial \hat{C}} = \frac{\hat{S}_xH(f)^2e^{-\hat{C}}}{(1+\hat{S}_xH(f)^2e^{-\hat{C}})} \ge 0 \tag{28c}$$

$$\lambda_c = \frac{\partial I[f,\hat{S}_x,\hat{C}]}{\partial \hat{C}} = \frac{\hat{S}_xH(f)^2e^{-\hat{C}}}{(1+\hat{S}_xH(f)^2e^{-\hat{C}})} \le 1 \tag{28d}$$

The bounds for $\{\lambda_c,\lambda_s\}$ follows from (28). □

In order to simplify notation we use the following definition:

$$\hat{Q} \triangleq \exp(-\hat{C}) \tag{29}$$

From (26b) It's clear that:

$$\hat{S}_x = \frac{\lambda_c}{\hat{Q}H(f)^2(1-\lambda_c)} \tag{30}$$

Substituting (30) in (26a) we get the following quadratic equation:

$$-H(f)^2(1-\lambda_c)\hat{Q}^2 + \left(H(f)^2 - \lambda_s - \lambda_cH(f)^2\right)\hat{Q} - \frac{\lambda_s\lambda_c}{1-\lambda_c} \tag{31}$$

Solving the quadratic equation that follows from (25) , we have two sets of solutions for $\{\hat{S}_x,\hat{Q}\}$ Define:

$$\psi_i = \begin{cases} 1 & i=1 \\ -1 & i=2 \end{cases} \tag{32}$$

$$X(f;\lambda_c,\lambda_s) \equiv H(f)^2 - \lambda_s - \lambda_cH(f)^2 \tag{33}$$

$$Q_i(f) = \tag{34}$$

$$= \frac{X(f;\lambda_c,\lambda_s) - \psi_i\sqrt{X(f;\lambda_c,\lambda_s)^2 - 4H(f)^2\lambda_c\lambda_s}}{2H(f)^2(1-\lambda_c)} \tag{35}$$

Inserting (34) into (30)

$$\hat{S}_{x,i} = \frac{2\lambda_c}{X(f;\lambda_c,\lambda_s) - \psi_i\sqrt{X(f;\lambda_c,\lambda_s)^2 - 4H(f)^2\lambda_c\lambda_s}} \tag{36}$$

Multiplying the denominator and numerator by $X(f;\lambda_c,\lambda_s) + \psi_i\sqrt{X(f;\lambda_c,\lambda_s)^2 - 4H(f)^2\lambda_c\lambda_s}$ will lead to the following solution

$$S_{x,i}(f) = \\ = \frac{X(f;\lambda_c,\lambda_s) + \psi_i\sqrt{X(f;\lambda_c,\lambda_s)^2 - 4H(f)^2\lambda_c\lambda_s}}{2H(f)^2\lambda_s} \tag{37a}$$

$$Q_i(f) = \\ = \frac{X(f;\lambda_c,\lambda_s) - \psi_i\sqrt{X(f;\lambda_c,\lambda_s)^2 - 4H(f)^2\lambda_c\lambda_s}}{2H(f)^2(1-\lambda_c)} \tag{37b}$$

Proposition 2. *Although equation (37) produce two curve sets,we discard the* $\{S_{x,2}(f), Q_2(f)\}$ *curve, since for each frequency (regardless of* $H(f)$*),* $I[f,\hat{S}_x,\hat{Q}]$ *is not concave in the pair* $\{S_{x,2}(f), Q_2(f)\}$*, meaning that one could improve the "optimal"* $I[f,\hat{S}_x,\hat{Q}]$ *simply by splitting the incremental frequency band.*

Proof. A rigorous proof can be found within 7.2. □

Hence the optimal curves for $S_x(f), Q(f)$ are:

$$S_x(f) = \frac{X(f;\lambda_c,\lambda_s) + \sqrt{X(f;\lambda_c,\lambda_s)^2 - 4H(f)^2\lambda_c\lambda_s}}{2H(f)^2\lambda_s} \tag{38a}$$

$$Q(f) = \frac{X(f;\lambda_c,\lambda_s) - \sqrt{X(f;\lambda_c,\lambda_s)^2 - 4H(f)^2\lambda_c\lambda_s}}{2H(f)^2(1-\lambda_c)} \tag{38b}$$

In stark contrast to classical water-pouring [11] and [10], the optimal solution will be discontinuous frequently. An outstanding example is $H(f)$ constant over f, sufficient SNR and rather low C. In this case an attempt to use frequency-constant $S_x(f)$, $C(f)$ will place us in the non-concave region and a better performing solution will use only part of the available spectra to utilize the available bits better by transmitting less information about the channel noise, and since $C(f)$ and $S(f)$ will never fall gradually down to zero, the transition will have always an abrupt part.

Figure 6 Information rate as a function of allocated bandwidth

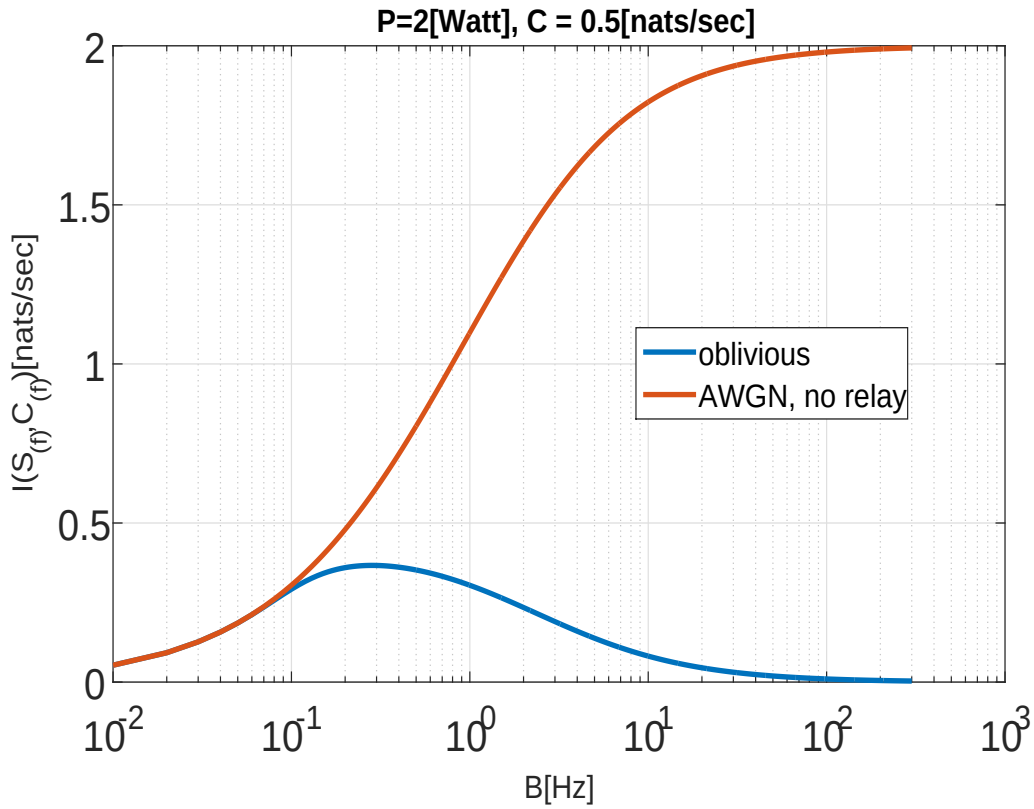

Figure 6 demonstrates this idea. Assuming a flat channel(i.e $H(f) = 1$). For a given total power $P = 2[Watt]$ and capacity $C = 0.5[nats/sec]$ we calculated the Mutual Information Rate when distributing the power and bit-rate uniformly over the bandwidth B.

$$I\left[S_x(f), C(f)\right] = B \log \left[\frac{1 + P/B}{1 + P/Be^{\frac{-C}{B}}} \right] \tag{39}$$

It is clear that the best course would not be to spread the power and bit-rate all over the spectrum.

5 Numerical Analysis

The algorithm has been tested for different types of channels(assigned as "Channel A") of the form $H_A(f) \equiv \alpha_1 N(f_1, 1) + \alpha_2 N(f_2, 1)$ (when $N(\mu, \sigma^2)$ is the Gaussian curve) with $P = 100, C = 9[nats/sec]$.We also tested the "reciprocal" channel - assigned as "channel B" (i.e, $H_B(f) = max[H_A(f)] - H_A(f)$) In each scenario, we've compared the overall information rate using the following algorithms:

- The proposed algorithm
- Uniform allocation of rate and power
- Classical water pouring as presented in [3], for the case of $C \to \infty$
- "Limited Rate Water Pouring", which is:
  A. Calculate $S_x(f)$ using the classical water pouring approach.
  B. The allocated rate is: $C(f) = \frac{C}{P} S_x(f)$

The results are summarized at the next figures and table. Each figure contains

a Normalized curves of $S_x(f), C(f)$ of the proposed algorithm with respect to $H(f)$

b Comprasion between the allocated power using the proposed approach and the classical water pouring

Figure 7 $\alpha_1 = 0.25, f_1 = 0.25W, \alpha_2 = 0.25, f_2 = 0.75W$

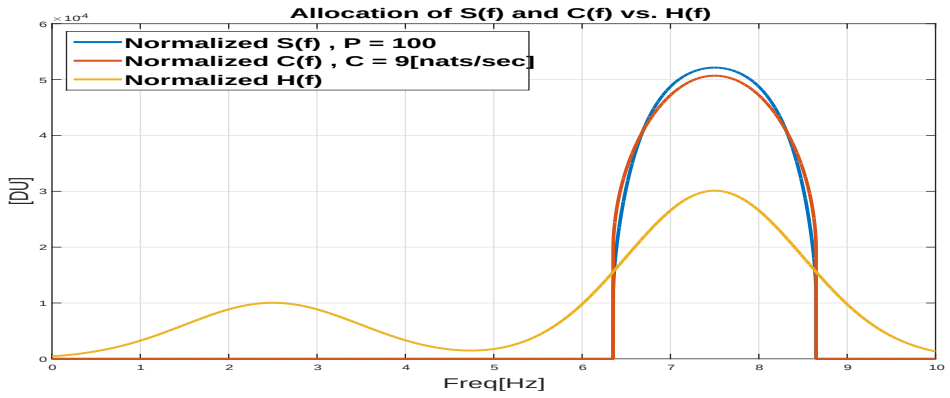

(a)

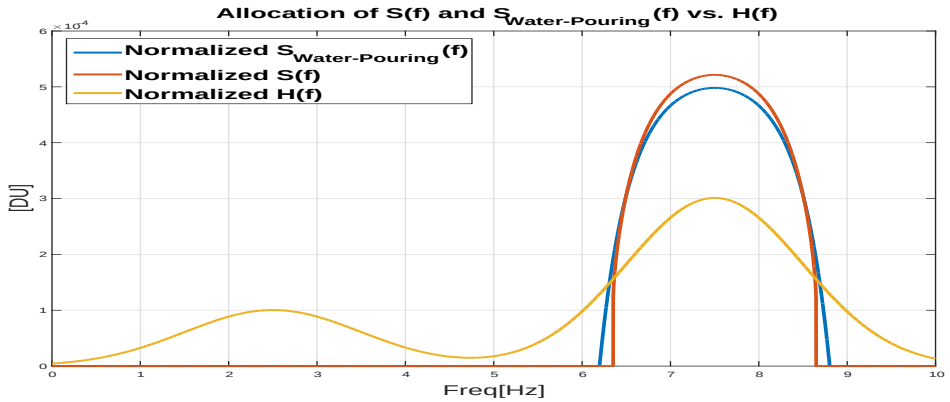

(b)

Figure 8 $\alpha_1 = 0.25, f_1 = 0.25W, \alpha_2 = 0.25, f_2 = 0.75W$, *Inverse Channel*

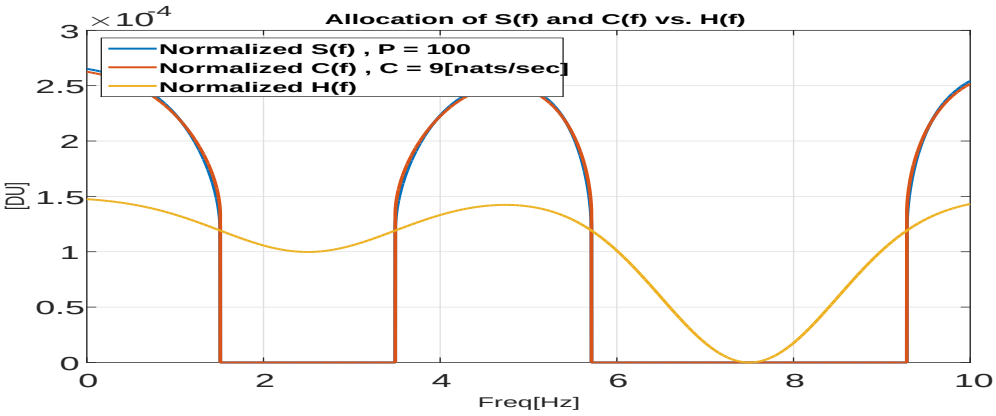

(a)

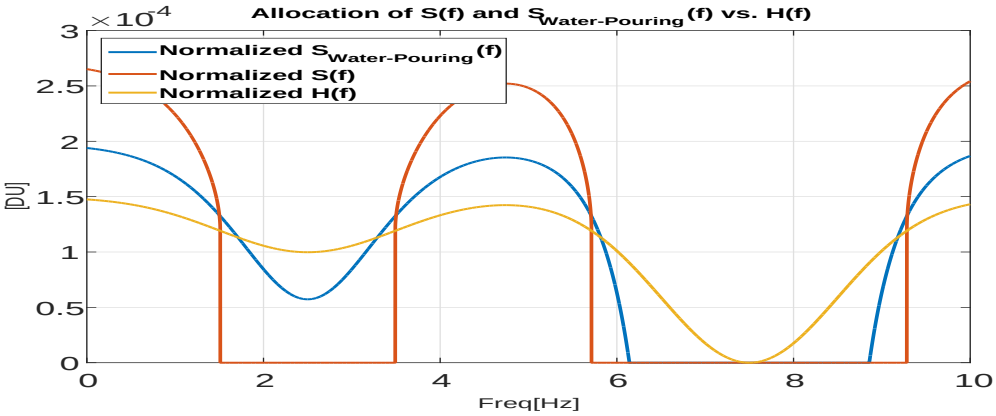

(b)

Figure 9 $\alpha_1 = 0, f_1 = 0, \alpha_2 = 1, f_2 = 0.5W$

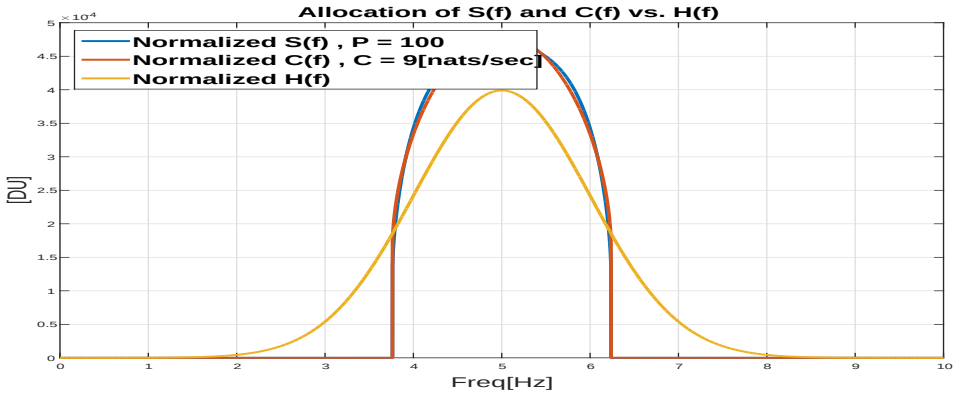

(a)

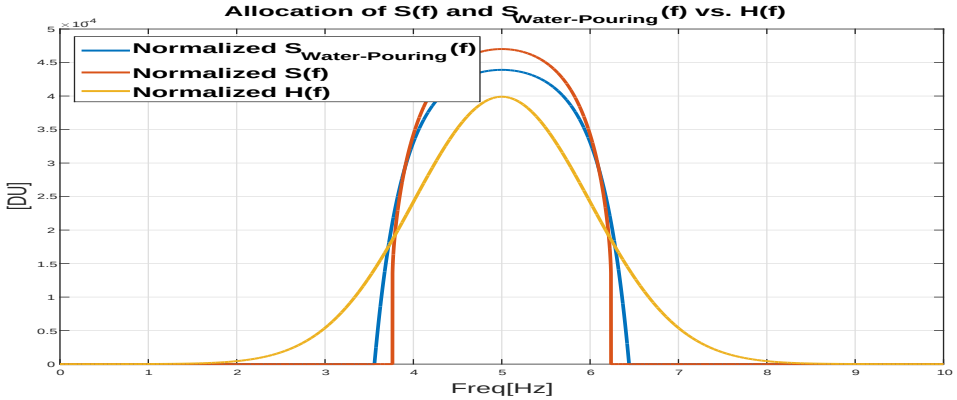

(b)

Figure 10 $\alpha_1 = 0, f_1 = 0, \alpha_2 = 1, f_2 = 0.5W$ *Inverse Channel*

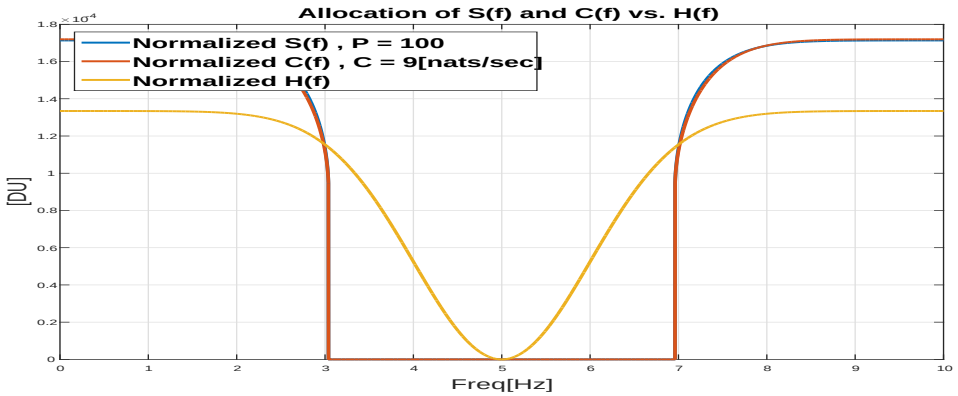

(a)

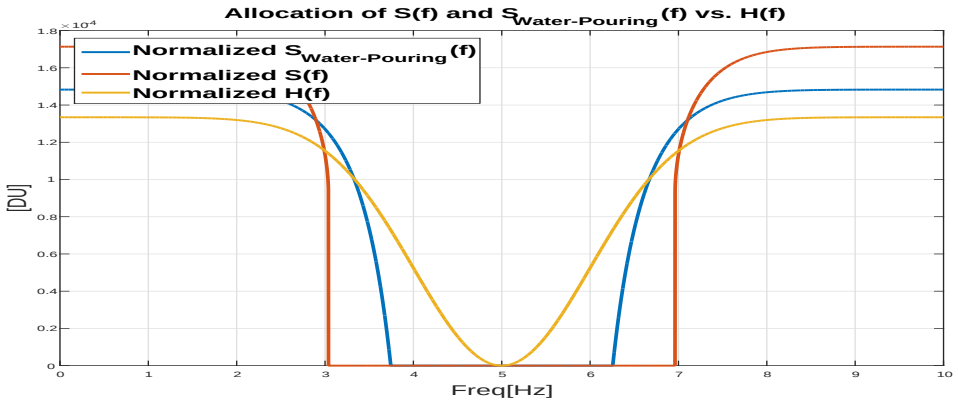

(b)

Figure 11 Uniform Channel

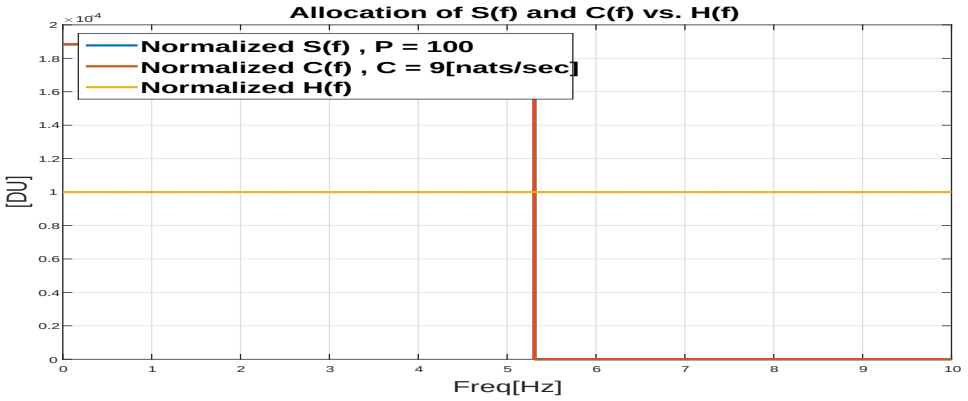

(a)

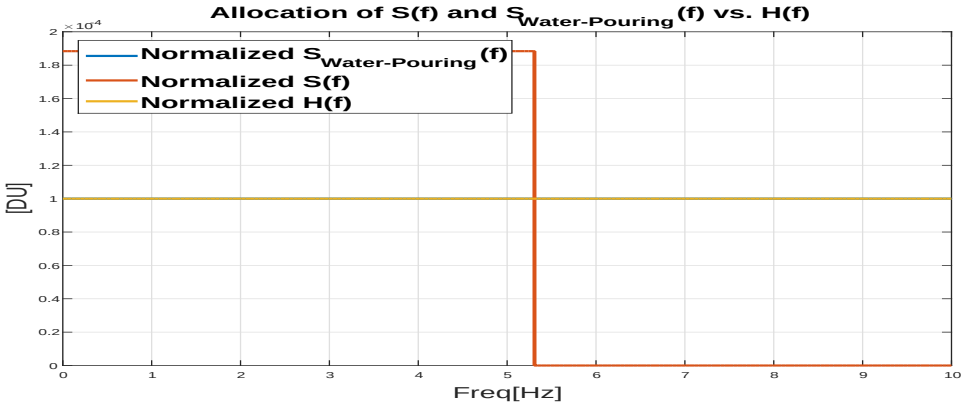

(b)

Case	α_1	f_1	α_2	f_2	Remark	$I_n^C(x,z)$	$I_n^\infty(x,z)$	$I_n^C(x,z)$ - Uniform Allocation	$I_n^C(x,z)$ - Limited Rate Water Pouring
1	0.25	$0.25W$	0.75	$0.75W$	Channel A , Fig. 7	2.83	2.94	0.77	2.80
2	0.25	$0.25W$	0.75	$0.75W$	Channel B , Fig. 8	3.40	4.53	1.98	3.03
3	0	0	1	0.5W	Channel A , Fig. 9	3.73	3.98	0.98	3.68
4	0	0	1	0.5W	Channel B , Fig. 10	4.98	7.85	3.28	4.62
5	-	-	-	-	Allpass , Fig. 11	7.92	23.98	7.75	7.75

Table 1: Comparison Between Channels (all units are [nats/sec])

It is clear form the results that:

- The proposed approach for allocating the power $S_x(f)$ and rate $C(f)$ is indeed optimal and superior to the other methods that are presented. Evidently, the rate is upper bounded by the classical water pouring result($C \to \infty$). It is evident:

$$I_n^\infty(x,z) \geq I_n^C(x,z) \geq \\ I_n^C(x,z)|_{\text{Limited Rate Water Pouring}} \geq I_n^C(x,z)|_{\text{Uniform Allocation}} \tag{40}$$

- The price of obliviousness is demonstrated, as for a cognitive relay the reliable rate is $min(I_n^\infty(x;z), C)$, achieved by a relay that decodes the signal and transmits then the decoded information at the maximum allowable rate (C).

6 Conclusions and Future Directions

We presented and analyzed the rate and power limited oblivious relay over the frequency selective AWGN channel and derived the optimal transmit power spectral density and the optimal allocation of the relay bit-rate for Gaussian signaling. Our results relate directly to the classical water-pouring as well as to the the Gaussian bottleneck frameworks. The advantage of this approach over other methods was demonstrated. Our results apply directly also to the frequency dependent vector (MIMO) channels presented in figure 1 and in section 3 above. Such channels can be transformed

to a set of parallel independent channels [21] . Thus equation (37) and the optimization algorithms can be applied on those with no need of modification by considering those independent channels as occupying independent frequency bands. A modern implementation of such a MIMO system might use the OFDM framework in which the MIMO channel diagonalization is convenient to implement(see for example [22])

An area under current investigation is the Constrained $H(z)$ for general memoryless channels. Let us replace the constraint $I(y;z) \leq C$ by

$$H(z) \leq C \tag{41}$$

It should be emphasized that the entropy constraint is per *symbol*, In this case we can apply insights from the results of [23]. This will result in a universal compression scheme, where standard algorithms, as the Lempel-Ziv , Arithmetic coding and others can be applied [11]. This will also enforce z to a discrete alphabet since otherwise $H(z)$ is infinite. Open questions:

A. Is the curve of the maximal $I(x;z)$ as a function of the maximal permitted $H(z)$ concave? It is of cause concave if time sharing between two different quantizers is allowed.

B. In which cases does the optimal mapping $y \to z$ become deterministic? In some cases it is stochastic, for example if y is binary there are only two possible deterministic quantizers, one of which is $z = y$ and the other $z = const$. So $H(z)$ has only two possible values. In such cases the quantizer will be stochastic or time sharing between different deterministic quantizers will be used. With deterministic quantizer the scheme becomes similar to Lloyd quantizer concatenated with entropy compression but may be superior to it because the quantizer is optimized jointly for $I(x;z)$ and $H(z)$. On the other hand there is a trivial way to transfer any stochastic quantizer to a deterministic one if the $x \to y$ channel is an additive noise channel.

6.1 Achieving the optimal performance with no division to subbands

The system we introduced allows analysis of the optimal performance and is implementable by practical hardware. Still a simpler system free of the time consuming operation of dividing the signal into narrow sub-bands is desirable. We shall present next such a system which still achieves the full performance as analyzed above. Let's denote the modified water-pouring approach presented above as the sub-bands approach and the new system as the ?ISI? approach

We can modify the encoder in Figure 1 as follows:

Figure 12 The ISI approach

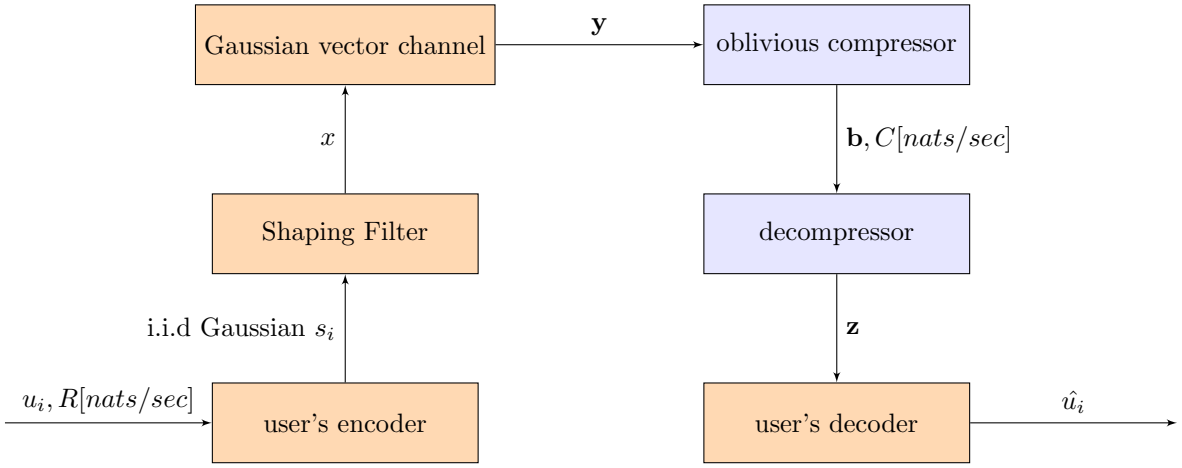

The information u_i is encoded into s_i by a Gaussian random codebook using symbol rate of s_i equal to the Nyquist rate of the channel. The resulting signal is spectrally shaped to achieve the optimal spectra identical to this of the subbands based system. This ISI based system achieves the same performance as the ?subbands ' based one because:

A. The Gaussian codebooks of the transmitted signals $x(t)$ in both the systems are identical.

B. The Compress block can forward $x(t)$ to the destination with the same performance as the subbands system.

The proof of the last two statements is included in the appendix.

A further step towards a practical system may be using the ISI approach and rendering the sampled signals at the receiver Gaussian i.i.d. so that scalar instead of vector compression is possible. This can be attempted using [24, 25, 26, 27] and [28]. Some of those approaches such as the MMSE-DFE approach in [25] require a Thomlinson-Harashima processing at the transmitter with some associated shaping loss. Dirty paper coding will probably perform with no loss. Another approach of rendering the signal i.i.d. is a linear orthogonalizing transform since the matched filter and sampler produce a vector of jointly Gaussian variables, and the singular value decomposition renders those independent, see [24] for such a decomposition.

7 Appendix

7.1 Proof of Theorem 1, independent z_i achieve the optimal performance

Define:

$$z_i \equiv (x_1^{i-1}, y_1^{i-1}, \mathbf{b}) \tag{42}$$

Since the code is unknown,x_i are independent and $x_i - y_i - z_i$ is a Markov chain. The variable z_i cannot be used directly in our scheme because it depends on x_1^{i-1} which are not available to the compressor and because they are dependent on each other. However the above Markov chain implies an existence of another random variable being a stochastic function of y_i only and having the same $P(x_i, y_i, z_i)$ and thus the same $I(x_i; z_i)$ and $I(y_i; z_i)$. The following equations analyze the properties common to z_i and to this other usable variable.

$$\begin{aligned} I(\mathbf{b}, \mathbf{x}) &= H(\mathbf{x}) - H(\mathbf{x}|\mathbf{b}) \\ &= \sum_{i=1}^{N} \left[H(x_i) - H(x_i|x_1^{i-1}, \mathbf{b})\right] \\ &\leq \sum_{i=1}^{N} \left[H(x_i) - H(x_i|x_1^{i-1}, y_1^{i-1}, \mathbf{b})\right] \\ &= \sum_{i=1}^{N} \left[H(x_i) - H(x_i|z_i)\right] \\ &= \sum_{i=1}^{N} I(x_i; z_i) \end{aligned} \tag{43}$$

Also:

$$\begin{aligned} \sum_{i=1}^{N} I(z_i; y_i) &\leq \sum_{i=1}^{N} I(z_i; y_i|x_1^{i-1}, y_1^{i-1}) \\ &= \sum_{i=1}^{N} I(x_1^{i-1}, y_1^{i-1}, \mathbf{b}; y_i|x_1^{i-1}, y_1^{i-1}) \\ &= \sum_{i=1}^{N} I(\mathbf{b}; y_i|x_1^{i-1}, y_1^{i-1}) \\ &\leq \sum_{i=1}^{N} I(\mathbf{b}; y_i, x_i|x_1^{i-1}, y_1^{i-1}) \\ &= I(\mathbf{b}; \mathbf{y}, \mathbf{x}) \\ &\leq H(\mathbf{b}) \\ &= N \cdot C \end{aligned} \tag{44}$$

The first line is because x_1^{i-1}, y_1^{i-1} has no information about y_i. The last two equations without the intermediate steps are:

$$\begin{aligned} \sum_{i=1}^{N} I(x_i; y_i) &\geq I(\mathbf{b}; \mathbf{x}) \\ \sum_{i=1}^{N} I(z_i; y_i) &\leq H(\mathbf{b}) = N \cdot C \end{aligned} \tag{45}$$

From $P(\mathbf{z}, \mathbf{x}, \mathbf{y})$ compute the N possibly distinct distributions $P_i(z_i, x_i, z_i)$. Those surely conform to (45). To acquire a single equivalent distribution $P^*(z^*, x^*, y^*)$, let s be a random variable distributed uniformly over $\{1, \ldots, N\}$, and let $z^* = (z_s, s), x^* = x_s, y^* = y_s$. We have:

$$\begin{aligned} I(x^*; z^*) &= I(x_s; z_s, s) = \\ &= I(x_s; s) + I(x_s; z_s|s) = 0 + \frac{1}{N} \sum_{i=1}^{N} I(x_i; z_i) \end{aligned} \tag{46}$$

Note that s in $I(x_s; z_s, s)$ is a random variable while i in the last sum is a known running index.

Thus, following (45), there exists a scalar random variable z^* such that:

$$N \cdot I(x^*; z^*) \geq I(\mathbf{b}; \mathbf{x}) \tag{47}$$
$$N \cdot I(y^*; z^*) \leq H(\mathbf{b}) = N \cdot C$$

The Markov property is preserved for $x^* - y^* - z^*$. Also $P(x^*, y^*) = P(x_i, y_i)$ because $P(x_i, y_i)$ doesn't depend on i. But with (47) we have an achievability scheme based on source coding and presented as the stochastic quantizer scheme above using $P^*(z^*, x^*, y^*)$.

7.2 Proof of Proposition 2

In this subsection we prove that we can discard the solution $\{S_{x,2}(f), Q_2(f)\}$ of (37). Since we are dealing with a single frequency so $H(f)$ is constant and its influence is only a scaling of $S(f)$. Let us rewrite the Lagrangian at (24)

$$L = log\left(\frac{1+S}{1+Se^{-C}}\right) - \lambda_s S - \lambda_c C \tag{48}$$

equation (37) becomes (remembering that $Q \triangleq e^{-C}, C = -log(Q)$):

$$S = \frac{1 - \lambda_c - \lambda_s + \psi_i\sqrt{(1-\lambda_c-\lambda_s)^2 - 4\lambda_c\lambda_s}}{2\lambda_s} \tag{49a}$$
$$Q = \frac{1 - \lambda_c - \lambda_s - \psi_i\sqrt{(1-\lambda_c-\lambda_s)^2 - 4\lambda_c\lambda_s}}{2(1-\lambda_c)} \tag{49b}$$

We can also write λ_s, λ_c as function of (S, Q)

$$\lambda_c = \frac{SQ}{1+SQ} \tag{50a}$$
$$\lambda_s = \frac{1}{1+S} - \frac{\lambda_c}{S} \tag{50b}$$

We'd like to choose the concave solution only, that is choose S, C

$$\frac{\partial^2 I}{\partial S^2}\frac{\partial^2 I}{\partial C^2} - \frac{\partial^2 I}{\partial S \partial C}\frac{\partial^2 I}{\partial C \partial S} \geq 0 \tag{51a}$$
$$\frac{\partial^2 I}{\partial S^2} \leq 0 \qquad and \qquad \frac{\partial^2 I}{\partial C^2} \leq 0 \tag{51b}$$

We than prove that region of value of Ψ_i and concavity overlaps.

Lemma 1. *Different ψ_i in (49) enforce different (S, C).*

Proof. Each (S, C) pair corresponds by (50) to a unique (λ_s, λ_c). Thus, the same (S, C) cannot be the outcome of two distinct (λ_s, λ_c) with different ψ. □

The next step will be to show that the lines $S(\lambda_s, \lambda_c) = f(C; \lambda_s, \lambda_c)$ that splits the regions of concavity and the sign of ψ coincide. Let's derive the dividing line between the $\pm$ regions in (49). At the dividing line $(1 + \lambda_c + \lambda_s)^2 - 4\lambda_c\lambda_s$ must be zero by the proof of lemma 1 and the and the fact the the functions are continuous, so at any point, the dividing line must be the result of (49) regardless of the value of ψ. Particularly: two points infinitesimally near and each on a different side of the dividing line have the same S, C in the limit and on the other hand also the same (λ_s, λ_c) by (50), so in the limit the value of ψ won't matter.

$$(1 - \lambda_c - \lambda_s)^2 - 4\lambda_c\lambda_s = 0 \tag{52}$$

leading to:

$$\lambda_{s,i} = (\lambda_c + 1) + \eta_i\sqrt{4\lambda_c} \tag{53}$$

where:

$$\eta_i = \begin{cases} 1 & i = 1 \\ -1 & i = 2 \end{cases} \tag{54}$$

Substituting back (53) into (49) yields:

$$S_i = \frac{1 - \lambda_{s,i} - \lambda_c}{2\lambda_{s,i}} = \frac{\lambda_c + \eta_i\sqrt{\lambda_c}}{\lambda_c + 1 + 2\eta_i\sqrt{\lambda_c}} \tag{55}$$

The allocated power S_i must be non-negative, hence by elimination, we discard η_1

$$S_{plus/minus} = \frac{-(\lambda_c - \sqrt{\lambda_c})}{\lambda_c + 1 - 2\sqrt{\lambda_c}} = \frac{\sqrt{\lambda_c}}{1 - \sqrt{\lambda_c}} \tag{56}$$

Remembering that $Q = \frac{1}{S}\frac{\lambda_c}{1-\lambda_c}$ and $C = -log(Q)$ we plot the curve $(S(\lambda_c), C(\lambda_c))$ which is exactly the line at fig. 13.

We now examine the concavity regions of (51), We use the following derivatives:

$$\frac{\partial^2 I}{\partial S^2} = -\frac{1}{(1+S)^2} + \frac{e^{-2C}}{(1+Se^{-C})^2} = -\frac{1}{(1+S)^2} + \frac{\lambda_c}{S^2} \tag{57a}$$

$$\frac{\partial^2 I}{\partial C^2} = \frac{S^2 e^{-2C}}{(1+Se^{-C})^2} - \frac{Se^{-C}}{1+Se^{-C}} = \lambda_c^2 - \lambda_c \tag{57b}$$

$$\frac{\partial^2 I}{\partial S \partial C} = \frac{\partial^2 I}{\partial C \partial S} = -\frac{Se^{-2C}}{(1+Se^{-C})^2} + \frac{e^{-C}}{1+Se^{-C}} = \frac{1}{S}(\lambda_c^2 - \lambda_c) \tag{57c}$$

It is easy to see that $\frac{\partial^2 I}{\partial S^2} < 0$ and $\frac{\partial^2 I}{\partial C^2} < 0$, we need to examine the sign regions of $\frac{\partial^2 I}{\partial S^2}\frac{\partial^2 I}{\partial C^2} - \frac{\partial^2 I}{\partial S \partial C}\frac{\partial^2 I}{\partial C \partial S}$ Substituting () in (51) we get:

$$0 = \frac{\partial^2 I}{\partial S^2}\frac{\partial^2 I}{\partial C^2} - \frac{\partial^2 I}{\partial S \partial C}\frac{\partial^2 I}{\partial C \partial S} = \tag{58a}$$

$$= \Big[-\frac{1}{(1+S)^2} + \frac{\lambda_c}{S^2} \Big] \Big[\lambda_c^2 - \lambda_c \Big] - \Big[\frac{1}{S}(\lambda_c^2 - \lambda_c) \Big]^2 \tag{58b}$$

Equation (58) leads to the following quadratic equation in S

$$S^2(\lambda_c - 1) + 2S\lambda_c + \lambda_c = 0 \tag{59}$$

Once more, we get to solution:

$$S_i = \frac{\lambda_c + \eta_i \sqrt{\lambda_c}}{1-\lambda_c} = \frac{\sqrt{\lambda_c}(\sqrt{\lambda_c} + \eta_i)}{1-\lambda_c} \tag{60}$$

We can discard $\eta_2(-)$ in order to ensure non-negative solution for S_i leading to:

$$S_{concave/convex} = \frac{\sqrt{\lambda_c}}{1-\sqrt{\lambda_c}} \tag{61}$$

We proved that regions of sign of ψ and concavity/convexity regions of (S, C) overlaps (Since λ_c determines the same unique S in both cases and (λ_c, S) determine a unique C.

A numerical simulation of this phenomena can easily demonstrated. we start by the following algorithm:

Algorithm 1 Calculate concavity/sign regions

- Choose a square domain of S, C
- Calculate λ_s, λ_c by 50
- Choose the correct sign function Ψ_i in order to get back S, C
- Once the sign is set, test for concavity

Figure 13 Concavity and sign regions

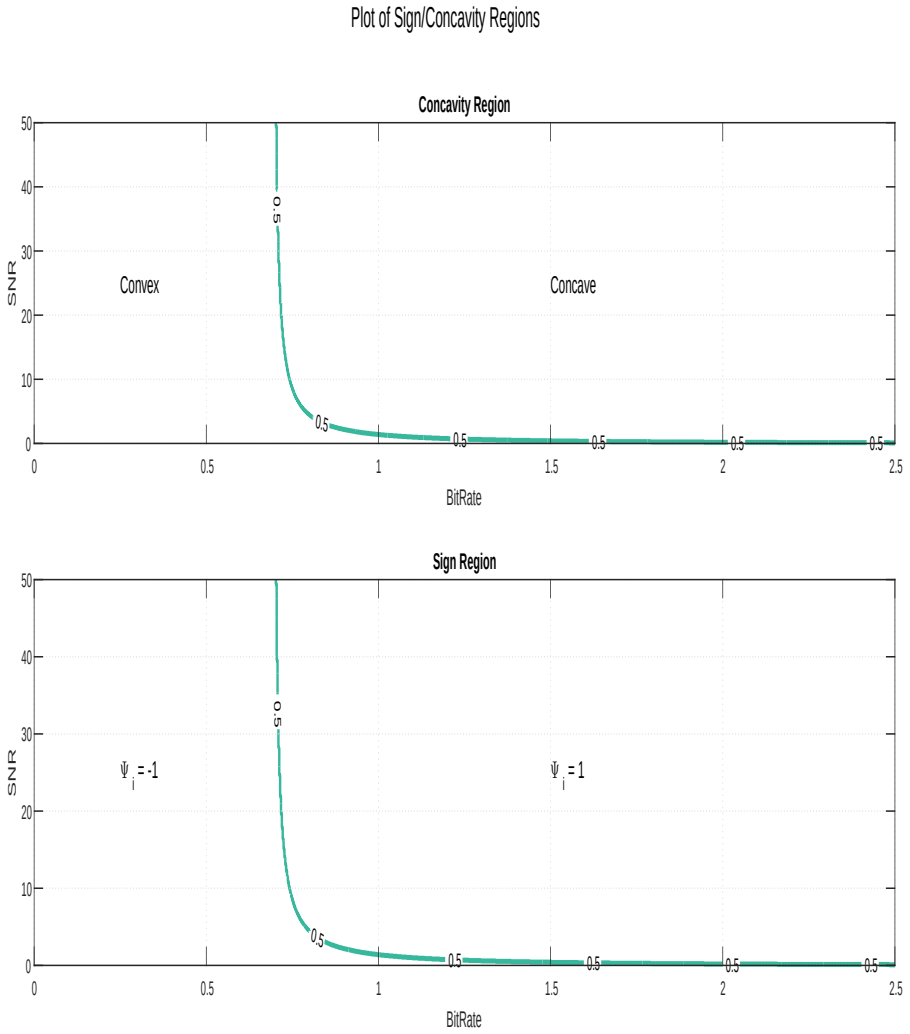

Figure 14 Unified plot of concavity/sign regions

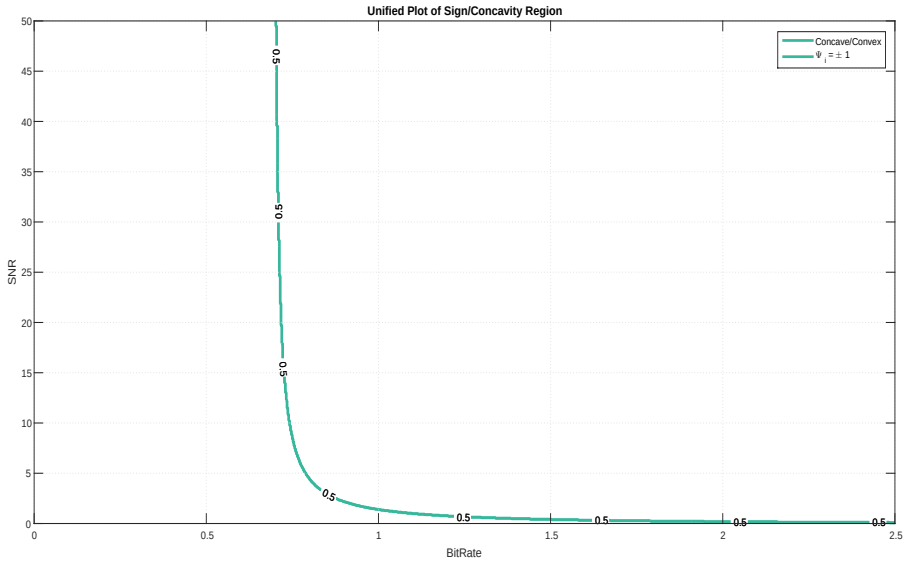

Figures 13 and 14 shows that the regions of concavity and sign overlaps. In this case we choose for the plus sign in order to get concave solution.

To conclude, let us investigate the lower limit on C using (56).

$$Q = \frac{1}{S} \cdot \frac{\lambda_c}{1-\lambda_c} = \frac{\sqrt{\lambda_c}}{1+\sqrt{\lambda_c}} \tag{62}$$

Hence:

$$\lim_{\lambda_c \to 1} C = \lim_{\lambda_c \to 1} -log(Q) = log(2) \tag{63}$$

This is the analytic derivation of the $1[bits/Hz]$ limit.

7.3 Discrete z suffices if y is discrete

[29, Lemma 2] can be rephrased as: Let $\mathbf{r}$ be any subset of R^n comprising at most k connected subsets. Let $P(\mathbf{r})$ be the PDF of $\mathbf{r}$ and define k functions $f_j(\mathbf{r}), j = 1 \dots k$. Then one can find k points $\mathbf{r_i}$ in $\mathbf{r}$ and assign them new probabilities q_i so that for each function:

$$E(f_j) = \sum_{i=1}^{k} q_i f_j(\mathbf{r_i}) \tag{64}$$

Where the expectation E is over the original continuous PDF. Now to our bottleneck problem: Suppose we found an optimal solution $P(z|y), y$ is discrete with N possible values denoted y_n and z is continuous. This mean we have the full statistics $P(x, y, z)$ defined by the set $P(x), P(y|x), P(z|y)$. This set can be transformed to the equivalent set $P(z), P(x|y), P(y|z)$. Invoke the above lemma with $z = \mathbf{r}$ with all the following expectations E defined over z. Continue as in [29, page 4]: Define the set of functions $\{f_j(z)\}_{j=1}^{N+1}$:

$$f_j(z) = \begin{cases} P(y = y_j|z) & 1 \le j \le N-1 \\ \sum_n P(y = y_n|z) log\left[P(y = y_n|z)\right] & j = N \\ \int_x P(x|z) log\left[P(x|z)\right] dx & j = N+1 \end{cases} \tag{65}$$

According to the set of functions $\{f_j(z)\}_{j=1}^{N+1}$ defined in (65) we have:

$$E(f_j) = \begin{cases} P(y = y_j) & j \le N-1 \\ H(y|z) & j = N \\ H(x|z) & j = N+1 \end{cases} \tag{66}$$

By the lemma above we can find $N+1$ points z_i and assign them probabilities $P(z_i)$ so that the following are preserved: $P(y)$ and so $P(x), H(y|z), H(x|z)$, thus the discrete z achieves the same bottleneck performance as the continuous one.

7.4 Optimality of the ISI approach

7.4.1 Proof of the identical codebooks

Shannon's random coding argument is based on a codebook of waveforms (signals of duration equal to the length of the transmitted block) drawn randomly from a random Gaussian process. Such a process is characterized fully by its Power Spectral Density (PSD). The transmitted signals in both the systems have the same PSD by design, so we have merely to show that they are Gaussian Stationary Random Process (GSRP). This is easy since with the subband approach the transmitted signal in each subband is GSRP and a sum of GSRPs is a GSRP. With the ISI approach the transmitted signal before the shaping filter is a frequency-flat GSRP, after the linear shaping filter it is still GSRP as well known.

7.4.2 Proof of identical compression performance at the relay

Let's consider the ISI based system. Since the noise is spectrally flat, the received signal can be first converted into a sufficient statistics by matched filtering (MF) and sampling at the symbol rate as shown for channels with ISI by Erickson [30] in 1971 and Forney [31] in 1972. Such sampled signals are jointly Gaussian random variables and those can be optimally compressed as Gaussian vectors, see [Tishbi]. A remark: Since we are sampling at Nyquist rate, any filter with $|H(f)| > 0$, not only MF, will do. Now consider the subbands system. The relay samples the received signal at Nyquist rate and then partitions it into subbands by linear filtering. We can insert the matched filter above before the sampler since it does not change the signal in each subband except for scaling which is irrelevant to the compression performance. Thus the signals to be compressed in both the systems differ just by a linear transformation converting each one into the other. Since the compression scheme of Tishbi [13] is optimal in the vector and in the scalar cases and since a linear transform is a permissible action of the vector compression scheme, the performance, quantified by the MUI as presented above, is identical.

Acknowledgement

This project has received funding from the European Union's Horizon 2020 Research And Innovation Programme under grant agreement no. 694630.

References

[1] Shamai S., Steinberg Y., Sanderovich A., and Kramer G. Communication via decentralized processing. *IEEE Trans. Information Theory*, 54(7):3008–3023, jul 2008.

[2] A. Globerson G. Chechik, Y. Weiss and N. Tishbi. Information bottleneck for gaussian variables. *Machine Learning Research*, 6:165–188, jan 2005.

[3] C.E. Shannon. Communication in the presence of noise. *Proc. IRE*, 37(1):10–21, jan 1949.

[4] A. Sanderovich, S. Shamai, and Y. Steinberg. Distributed mimo receiver-achievable rates and upper bounds. *IEEE Trans. Information Theory*, 55(10):4419–4438, oct 2009.

[5] A. Winkelbauer and G Matz. Rate-information-optimal gaussian channel output compression. *48th Annual Conference on Information Sciences and Systems (CISS),*, (1-5), aug 2014. doi: 10.1109/CISS.2014.6814120.

[6] S. Farthofer A. Winkelbauer and G. Matz. The rate-information trade-off for gaussian vector channels. *IEEE International Symposium on Information Theory (ISIT)*, pages 2849 – 2853, jul 2014.

[7] T. Berger. *Rate-Distortion Theory*. Wiley Online Library, 2003.

[8] R. Dobrushin and B. Tsybakov. information transmission with addi- tional noise. *IRE Transactions on Information Theory*, 8(5):293–304, 1962.

[9] A. Kipnis, A.J. Goldsmith, Y.C. Eldar, and T. Weissman. Distortion-rate function of sub-nyquist sampled gaussian sources. *IEEE Transactions on Information Theory*, 62:401–429, Jan 2016.

[10] A. Kipnis, Y.C. Eldar, and A.J. Goldsmith. Sampling stationary signals subject to bitrate constraints. *arXiv:1601.06421*, 2016.

[11] T. M. Cover and J. A. Thomas. *Elements of Information Theory*. Elements in Communications and Signal Processing. Wiley, tenth edition, aug 1991.

[12] J. Singh, O. Dabeer, and U. Madhow. Capacity of the discrete-time awgn channel under output quantization. *IEEE International Symposium on Information Theory*, pages 1218–1222, july 2008.

[13] G. Chechik, A. Globerson, N. Tishby, and Y. Weiss. Information bottleneck for gaussian variables. *Journal of Machine Learning Research*, (6):165–188, 2005.

[14] T. Koch. On the capacity of the dither-quantized gaussian channel. *IEEE International Symposium on Information Theory (ISIT)*, 2014. arXiv:1401.6787.

[15] A. Globerson and N. Tishbi. On the optimality of the gaussian information bottleneck curve. *Unpublished*, 2003. HUJI TR.

[16] H. S. Witsenhausen and A. D. Wyner. A conditional entropy bound for a pair of discrete random variables. *IEEE Trans. Information Theory*, 21(5):493–501, sept 1975.

[17] N. Tishbi, F. Pereira, and W. Bialek. Information bottleneck method. *Proc. 37th Allerton Conf. on Communication, Control and Computing*, pages 368–377, sept 1999.

[18] S. Shamai D. Guo and S. Verdu. The interplay between information ans estimation measures. *Foundation and Trends in Signal Processing*, 6(4):243–429, 2012.

[19] R. G. Gallager. *Information Theory and Reliable Communications*. John Wiley, New York, 1968.

[20] I. M. Gelfand and S. V. Fomin. *Calculus of Variations*. Prentice-Hall, Englewood Cliffs, NJ, 1963.

[21] L. Brandenburg and A. Wyner. Capacity of the gaussian channelwith memory: The multivariate case. *Bell System Technical Journal*, 53:745–779, may 1974.

[22] J. Mietzner, R. Schober, L. Lampe, W. H. Gerstacker, and P. A. Hoeher. Multiple-antenna techniques for wireless communications - a comprehensive literature survey. *IEEE Communications Surveys & Tutorials*, 11(2), 2009.

[23] H. Gish and J.N. Pierce. Asymptotically efficient quantization. *IEEE Transactions on Information Theory*, 14(5):676–684, sep 1968.

[24] W. Hirt and J. L. Massey. Capacity of the discrete-time gaussian channel with intersymbol interference. *IEEE Trans. Inform. Theory*, 34(3):380–388, may 1988.

[25] M. V. Eyuboglu J. M. Cioffi, G. P. Dudevoir and G. D. Forney. Mmse decision-feedback equalizers and coding-part i: Equalization results, part ii: Coding results. *IEEE Trans. Communication*, 43(10):2582–2604, oct 1995.

[26] L. H. Ozarow S. Shamai (Shitz) and A. D. Wyner. Information rates for a discrete-time gaussian channel with intersymbol interference and stationary inputs. *IEEE Trans. Inform. Theory*, 37(6):1527–1539, nov 1991.

[27] S. Shamai (Shitz) and R. Laroia. The intersymbol interference channel: Lower bounds on capacity and precoding loss. *IEEE Trans. Inform. Theory*, 42(5):1388–1404, sep 1996.

[28] Yair Carmon and Shlomo Shamai. Lower bounds and approximations for the information rate of the isi channel. *arXiv:1401.1480*, jan 2014.

[29] M. Salehi. Cardinality bounds on auxiliary variables in multiple-user theory via the method of ahlswede and korner. *Standford, Technical report*, 33, aug 1978.

[30] T. Ericson. Structure of optimum receiving filters in data transmission systems. *IEEE Trans. Inform. Theory*, 17:353–353, may 1971.

[31] G. D. Forney. Maximum-likelihood sequence estimation of digital sequences in the presence of intersymbol interference. *IEEE Trans. Inform. Theory*, 18:363–378, may 1972.